euspen's 23rd International Conference & Exhibition, Copenhagen, DK, June 2023
www.euspen.eu

Indirect compensation strategy to minimise spatial thermal errors caused by activity of the milling machine rotary table

Daniel Divíšek[1], Martin Mareš[1], Otakar Horejš[1], Seung Min Jeong[2]

[1] *Czech Technical University in Prague, Faculty of Mechanical Engineering, Department of Production Machines and Equipment, RCMT, Horská 3, 128 00 Prague, Czech Republic*
[2] *DN Solutions, Haewon-ro, Seongsan-gu, Changwon-si, Gyeongsangnam-do, Korea*

D.Divisek@rcmt.cvut.cz

Abstract

Thermally induced errors are dominant sources of machine tool (MT) inaccuracy and are often the most difficult types of errors to reduce. Software compensation of thermally induced displacements at the TCP is a widely employed technique to reduce these errors due to its cost-effectiveness, minimal demands for additional gauges without structural modifications, energy savings, and ecology. Compensation models of MT thermal errors were successfully applied to various types of MT structure and production technologies and implemented directly into their control systems. This paper deals with the procedure for compensation of spatial themal errors caused by the rotary table activity of the milling machine. The aim is to develop an approach to extend the validity of the model calibrated at one point to the entire workspace of the machine.

Machine tool, Thermal error, Compensation, Rotary axis, Spatial accuracy

1. Introduction

The heat generated in the machine tool (MT) causes thermal expansion and bending of the machine parts. This problem can generally be solved in one of three ways [1]:

- design of symmetrical machine structure less sensitive to thermal effects (e.g. [2])
- design of the cooling system and its control (e.g. [3])
- thermal error compensation (e.g. [4])

Thermal error compensation methods can be divided further into [5]:

- direct compensation
- indirect compensation

Direct compensations are based on tool displacement measurements using tool or workpiece measuring probes. The advantage is knowledge of the deviations in real time, without the need to calibrate the mathematical model. However, the disadvantage is that the probes cannot continuously measure deviations during machining. Therefore, it is always necessary to interrupt the machining process for measurement. Interruptions affect the productivity of the MT, and thus increase the cost of the individual workpieces. The latest state-of-the-art in-process and on-machine measurement systems and sensor technologies is presented by Gao et al. in [6].

The basis of indirect compensation is a certain mathematical model mostly using measured inputs (e.g. structural and ambient temperatures, spindle speed, velocities, and other NC data). The model is generally calibrated in the non-production time of the machine; corrections at the tool centre point (TCP) are calculated in real time and send into MT control system in the form of offsets of movement axes. An detailed overview of approaches to thermal error modelling can be found in Mayr [7].

The most widespread methods of indirect compensation are:

- multiple regression analysis (MRA) (e.g. [8]);
- artificial neural networks (ANN) (e.g. [9]);
- finite element method (FEM) (e.g. [10]);
- transfer functions (TF) (e.g. [11]).

The strategy used in current research is an approach based on transfer function (TF) theory. Transfer function generally describes the relationship between the input (excitation) and output (response) of a dynamic system. In thermomechanical phenomenons the input is the temperature measured at the close to point of heat generation, and the output is the relative displacement measured between TCP and usual position of the workpiece (a rotary table in this case). The TFs respect principles of the heat transfer, have very good approximation properties and low requirements for additional sensors. Therefore, this versatile modelling approach can be applied to different types of MTs and production technologies [12].

The majority of thermal error compensation models determine the compensation values for the individual machine direction independently to TCP position in the MT working area due to the fact the models are usually calibrated for one configuration of MT axes (typically at the centre of the machine table). However, the inhomogeneous temperature field of the MT can cause different changes in the geometric accuracy dependent on time of the machine throughout the whole workspace (change in the spatial accuracy of the machine) [13].

Therefore, the development of an algorithm that extends the validity of the compensation model calibrated at one point to the whole working machine is the main focus of this article.

2. Experimental set-up and thermal error measurement

The tested machine was a five-axis vertical milling centre equipped with a rotary table (max 20 rpm).

Four precision datum balls mounted on a carbon-fiber composite bases with low thermal expansion coefficient (close to zero) were used as measurement artefacts. The artefacts were placed in the MT working space in positions visible in

Figure 1. Deviations from the refference positions of the datum balls were measured by a Renishaw RMP60 touch probe.

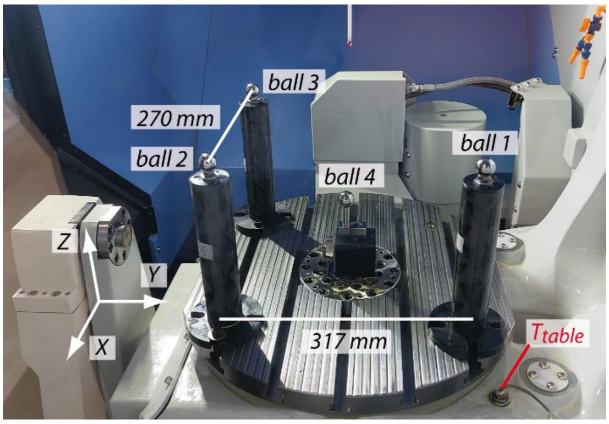

Figure 1.: Experimental set-up

An external temperature sensor T_{table} was placed on the machine surface near the rotary table bearings (position is visible in Figure 1). In addition, ambient temperature $T_{ambient}$ was measured in outer space of the MT

The experiment consists of two parts, a heating and a cooling phase. The testing procedure was repeated throughout the two cycles, a loading and a measurement. The loading cycle lasted for 23 minutes, followed by 7 minutes of measurement. Both cycles were repeated cyclically. During the loading cycle, the table was rotated about the C-axis at a set table speed (0 rpm in the cooling phase). During the measurement cycle, the table was stopped at the position C=0° and the tool probe measured the deviations from programmed positions of all the datum balls in the *X*, *Y,* and *Z* axes, respectively.

Two experiments were carried out with different table speed settings. Speed settings, along with measured temperature changes and measured deformations of datum balls over the time during the experiments can be seen in Figure 2. The experiment shown on the left of Figure 2 was used to develop the compensation model of thermally induced errors. The experiment on the right of Figure 2 is employed to verify the efficiency of the model. This paper focuses on minimisation of the *X*-axis thermal errors as the most complicated direction. The thermal error model of the *Y*-axis follows the introduced structure as well and the thermal deformations in the *Z*-axis cused by table rotation are not subject to compensation due to the neglected magnitude.

3. Model development

The compensation model for the X-axis is based on the TF principle. A discrete TF describing a link between the excitation and its response is expressed in the following equation.

$$y(t) = u(t) \cdot \varepsilon + e(t) \tag{1}$$

The vector $u(t)$ in eq. (1) is the TF input and $y(t)$ is the output vector in the time domain, ε represents the general TF in the time domain, and $e(t)$ is the disturbance value (further neglected). The difference form (suitable for programming languages, e.g. Python) of the TF in the time domain follows in eq. (2).

$$y(k) = \frac{u(k-n)a_n + \cdots + u(k-1)a_1 + u(k)a_0}{b_0} - \frac{y(k-m)b_m + \cdots + y(k-1)b_1}{b_0}, \tag{2}$$

where u is the TF input vector, y is the output vector, *k-n* (*k-m*) signifies the *n*-multiple (*m*-multiple) delay in sampling frequency. Linear parametric models of ARX (autoregressive with external input) identifying structure is used to set TF calibration coefficients a_n and b_m with the help of Matlab Identification Toolbox [14]. The ARX as an optimal model structure is also discussed in [15]

The compensation model is created for datum balls 1 – 3. The deformation measured on the datum ball 4 (central) is minimal

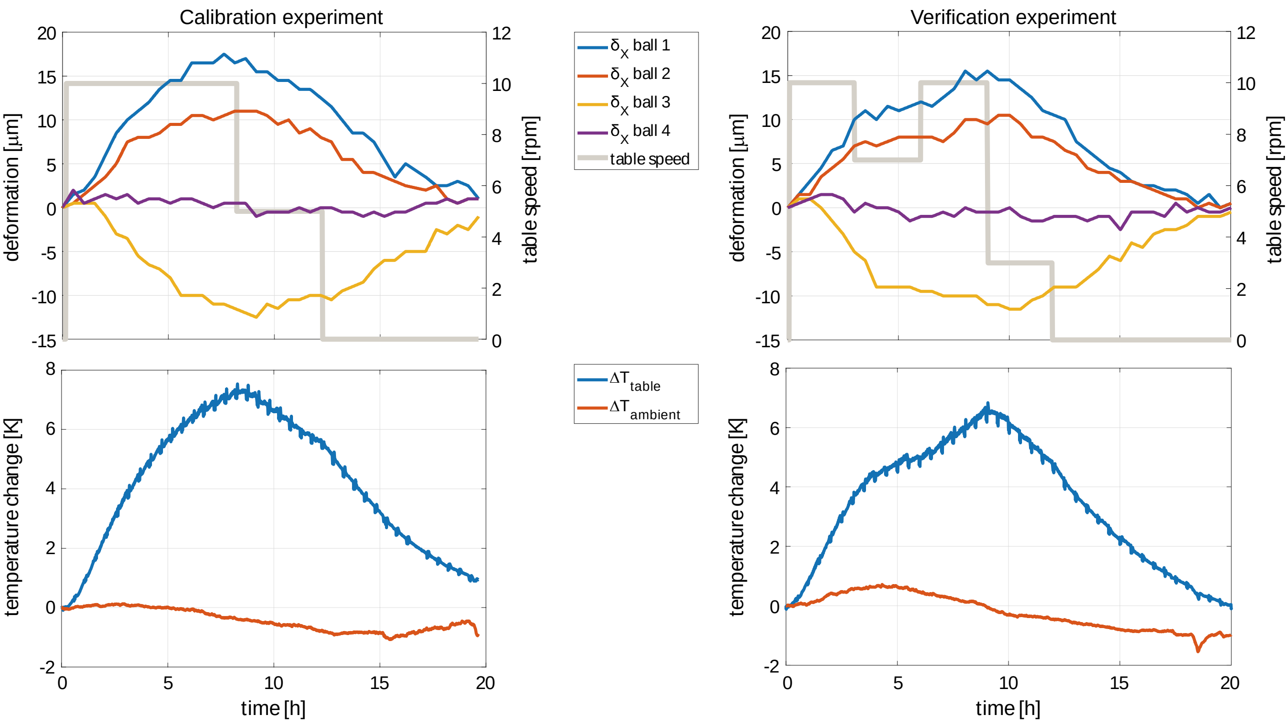

Figure 2.: Measured deformation, table speed profiles, and temperature during calibration (left) and verification (right) experiments

due to the table symmetry, and the datum ball 4 is from compensation effort excluded. The input in this case is the change of temperature T_{table} (ΔT_{table} as shown in Figure 2) and the output is the deformation of the datum ball 1.

The extension of the model to the entire workspace is performed by means of coefficients g_i depending on the $[X; Y]$ machine coordinates of the actual position of the TCP in the working area. The extension actually means a linear extrapolation of the model for datum ball 1 to the remaining three artefacts in order to obtain the best approximation of the measured deformations. Subsequently, the machine coordinates of each datum ball are rewritten in the format $[X_{ball};\ Y_{ball};\ g_i]$, where X_{ball} and Y_{ball} are the machine coordinates of the datum ball and g_i is the model extrapolation coefficient (gain). The basic model for the whole workspace is expressed in eq. (3).

$$\delta_{X_{SIM_1}} = \Delta T_{table} \cdot \varepsilon_{X_1} \cdot g_1 \tag{3}$$

The expression of the plane (determined from the three points) is given in eq. (4).

$$g_1 = \frac{255.644 \cdot X_{ball} + 47.25 \cdot Y_{ball} + 682.56}{42660}, \tag{4}$$

where g_1 is the extrapolation coefficient (gain) for TF1 into the whole working area and ε_{X_1} is the TF1 in the time domain (TF1 calibration coefficients are sumarised in Table 1).

However, the thermal erros in the X direction are not completely symmetrical. The deformations measured on datum ball 3 have a larger time constant compared to the other datum balls. For this reason, a second TF (TF2) is added to the compensation model to further enhance its accuracy (areas of validity of TF1 and TF2 are shown in Figure 3). The input to TF2 is unchanged to TF1, but the output is the deformation measured on the datum ball 3.

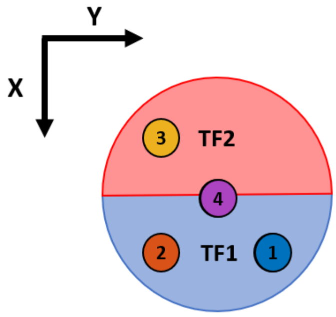

Figure 3.: Table division for TF application

The extended X-axis thermal error compensation model valid in the whole workspace is then expressed as follows

$$\begin{aligned} \delta_{X_{SIM_1}} &= \Delta T_{table} \cdot \varepsilon_{X_1} \cdot g_1 \\ \delta_{X_{SIM_2}} &= \Delta T_{table} \cdot \varepsilon_{X_2} \cdot g_2, \end{aligned} \tag{5}$$

where

$$g_2 = \frac{-386.784 \cdot X_{ball} + 64.8 \cdot Y_{ball} + 682.56}{42660} \tag{6}$$

is the extrapolation coefficient of TF2 and ε_{X_2} is the TF2 in the time domain to approximate datum ball 3 (TF2 calibration coefficients are summarised in Table 1).

Values of g_i extrapolation coefficients for $X_{ball} \in$ <-135;135> and $Y_{ball} \in$ <-158;158> are depicted in Figure 4.

Table 1.: Coefficients of identified transfer functions TF1 and TF2

TF	coefficients				
ε_{X_2}	a_0	a_1	a_2	a_3	a_4
	$-4.2 \cdot 10^{-7}$	0	0	0	0
	b_0	b_1	b_2	b_3	b_4
	1	-0.9996	-0.5	$-1.9 \cdot 10^{-4}$	0.4998
ε_{X_1}	a_0	a_1	a_2		
	0.0186	-0.0186	0		
	b_0	b_1	b_2		
	1	-1.9933	0.9933		

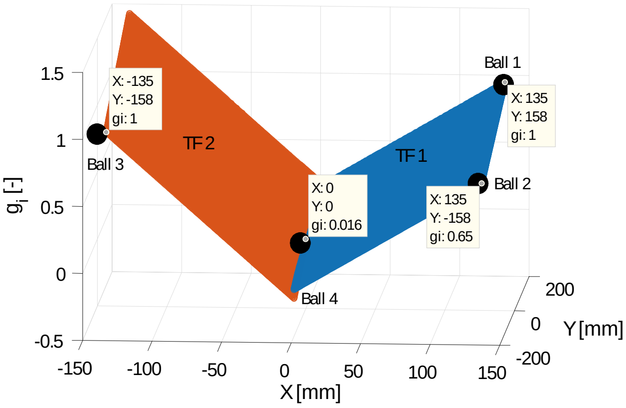

Figure 4. Values of the extrapolation coefficients g_i for the X-axis thermal error model extension into MT working area.

The results of the compensation models (basic form eq. (3) and extended form eq. (5)) built according to the above procedure during calibration test are shown in Figure 5.

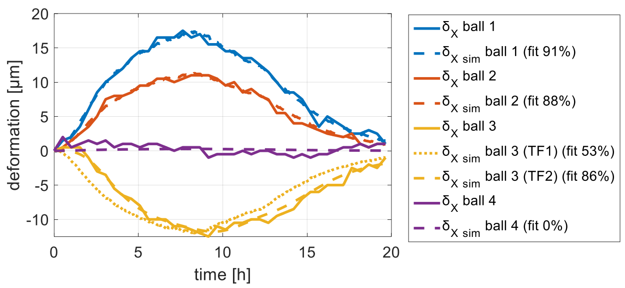

Figure 5. Measured and simulated deformations during calibration

The approximation quality of the simulated behaviour is expressed in eq. (7). The percentage *fit* value is based on the least square method where 100% would equal to a perfect match of the measured and simulated behaviours [14].

$$fit = \left(1 - \frac{\|\delta X_{MEA} - \delta X_{SIM}\|}{\|\delta X_{MEA} - \overline{\delta X_{MEA}}\|}\right) \cdot 100, \tag{7}$$

where δX_{MEA} is the measured output (thermal deformation in the X direction), δX_{SIM} is by model simulated output, and $\overline{\delta X_{MEA}}$ expresses the arithmetic mean over time of the measured output.

4. Model verification and results

The model described in Section 3 is validated on measured data from the verification test. Figure 6 shows a comparison of measured and simulated X-axis deformations for individual balls.

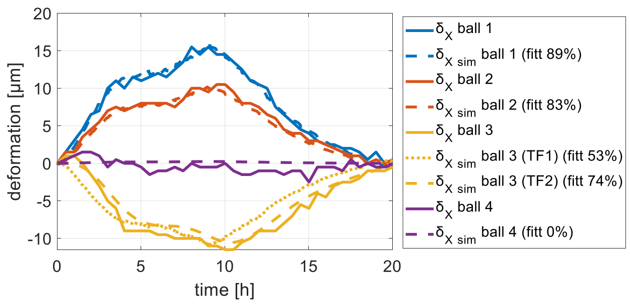

Figure 6. Comparison of measured and simulated deformations

The compensation results for individual artefact possitions are given in Table 3. A comparison between calibration and model verification is also provided. The results show sufficient accuracy and transferability of the model between operations with different table speed settings. Furthermore, the extension of the model to the form in eq. (5) respecting the non-symmetric thermal behaviour in the X direction enhanced the efficiency by 24% compared to the basic model in eq. (3).

Table 3.: Results of the thermal error compesation

		ball 1	ball 2	ball 3	ball 4
calibration	fit [%]	91	88	86	-
	max residue [µm]	1.6	1.1	1.5	2.0
verification	fit [%]	89	83	74	-
	max residue [µm]	1.6	1.4	2.9	2.6

The residual thermal error profiles for each datum ball (difference between measured and simulated deformations representing the MT state after compensation) are depicted in Figure 7.

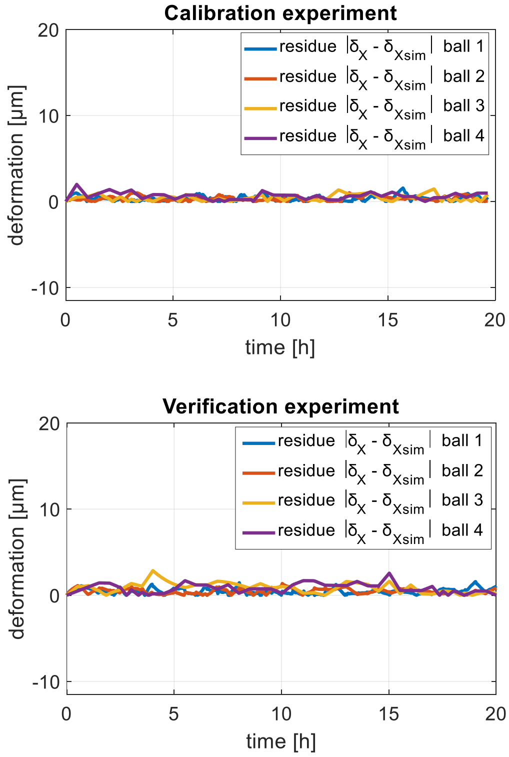

Figure 7. The residue profile for each datum ball during calibration (upper) and verification (lower) experiments.

5. Conclusion

Based on measured data on a five-axis vertical milling centre with a rotary table, a suitable mathematical compensation model was designed to approximate thermal deformations caused by table rotation. A strategy for minimisation of the thermal errors in the X direction throughout the MT working area was developed and the model was verified on an experiment with different table speed settings. Based on the verification, it can be concluded that the model is sufficiently effective to compensate up to 85% of thermal errors within specific working conditions.

Further research will focus on transferability of the proposed model to machines with similar design but upgraded to be capable of turning operations. Also, the inclusion of the cutting process and the process fluid needs to be considered.

Acknowledgement

This work was supported by the Grant Agency of the Czech Technical University in Prague, grant no. SGS22/159/OHK2/3T/12. The results are also obtained thanks to the previous funding support obtained within the project 'Machine Tools and Precision Engineering', reg. N° CZ.02.1.01/0.0/0.0/16_026/0008404.

References

[1] Weck M., et al., 1995, Reduction and compensation of thermal errors in machine tools, *Annals of the CIRP*, **44**(2), p. 589-598.

[2] Deng X.-L., et al., 2018 Review on thermal design of machine tool spindles, *Optics and Precision Engineering*, p. 1415-1429.

[3] Jedrzejewski J., et al., 2020, Research on Forced Cooling of Machine Tools and its Operational Effects, *Journal of Machine Engineering*, **20**(2), p. 18–38.

[4] Ramesh R., et al., 2000, Error compensation in machine tools - a review: Part II: thermal errors, *Int.J.Mach.Tools Manuf.*, **40**(9), p. 1257-1284.

[5] Brecher C., et al., 2010, Compensation of Thermo-Dependent Machine Tool Deformations Due to Spindle Load Based on Reduced Experimental Procedure and Modeling Effort – Synthesis Between Direct and Indirect Compensation, *8th International Conference on High Speed Machining*, Metz, France.

[6] Gao W., et al., 2019, On-machine and in-process surface metrology for precision manufacturing, *CIRP Annals*, **68**(2), p. 843-866.

[7] Mayr J., et al., 2012, Thermal issues in machine tools, *CIRP Ann.Manuf.Technol.*, **61**(2), p. 771–791.

[8] Naumann C., et al., 2020, Comparison of basis functions for thermal error compensation based on regression analysis – a simulation based case study, *Journal of Machine Engineering*, **20**(4), p. 28-40.

[9] Mize C., et al., 2000, Neural network thermal error compensation of a machining center, *Precision Engineering*, **24**, p. 338-346.

[10] Mayr J., et al., 2009, Compensation of thermal effects on machine tools using a FDEM simulation approach, *Proceedings Lamdamap*, **9**.

[11] Brecher C., et al., 2004, Compensation of thermo-elastic machine tool deformation based on control internal data, *CIRP Ann.Manuf.Technol.*, **53**(1), p. 299-304.

[12] Mareš M., et al., 2020, Thermal error minimization of a turning-milling center with respect to its multi-functionality, *Int. J. of Automation Technology*, **14**(3), p 475-483.

[13] Brecher C., et al., 2015, Control-Internal Compensation Algorithm for thermally induced volumetric Tool-Center-Point Deviations *Proceedings of Laser Metrology and Machine Performance XI.* Huddersfield, p. 1-11.

[14] Ljung L., 2015, System Identification Toolbox™ User's Guide, The MathWorks.

[15] Mayr J., et al., 2018, An adaptive self-learning compensation approach for thermal errors on 5-axis machine tools handling an arbitrary set of sample rates, *CIRP Annals - Manufacturing Technology*, p. 551-554.